Phase diagrams for coupled spin-gauge systems

Michael Creutz
Department of Physics, Brookhaven National Laboratory, Upton, New York 11973
(Received 27 August 1979)

Using Monte Carlo techniques, we study Z_N lattice gauge theory coupled to a Higgs field represented by spins situated on the lattice sites. We present phase diagrams for the Z_2 and Z_6 theories with the Higgs field in the fundamental representation of the gauge group and for Z_6 gauge theory coupled to Z_3 Higgs fields.

I. INTRODUCTION

Recent results establish the utility of Monte Carlo procedures for the study of phase transitions in lattice gauge theory.[1-3] Here we extend those investigations to coupled spin-gauge systems. Placing spins on lattice sites provides a prototype for a matter field which can produce gauge-meson masses via the Higgs mechanism.[4] This system carries two coupling constants, β corresponding to the gauge-field self-interaction and β_H representing the strength of the nearest-neighbor gauge-invariant spin-spin interaction. For large β the gauge fields become ordered and the model reduces to a conventional nearest-neighbor spin system exhibiting the ferromagnetic transition responsible for the Higgs mechanism. For vanishing β_H the site spins disorder and the model reverts to the pure gauge theory. Depending on the gauge group and the dimensionality of space-time, there may be one or more phase transitions along this line.[1-3,5]

Several authors have discussed phase diagrams for these systems.[6] When the site spins are in the fundamental representation of the gauge group G, the ordered spin phase of the Higgs mechanism is analytically connected to the disordered phase of the pure gauge field. When the spins are in another representation R, the theory at large β_H reduces to a pure gauge theory with group G/R, i.e., the subgroup of G under which the matter fields are invariant. In this case the above-mentioned phases can be distinct. In this paper we use Monte Carlo techniques on a four-dimensional lattice to "experimentally" confirm this structure. We restrict our treatment to the discrete Abelian gauge groups Z_N.

In the next section we define the models and summarize the Monte Carlo procedure. In Sec. III we discuss the limiting regions bounding the phase diagram. Section IV contains the phase diagrams for Z_2 and Z_6 gauge fields. For Z_6 we consider matter fields in both Z_6 and Z_3. The latter case gives a nontrivial quotient group $Z_6/Z_3=Z_2$. Section V contains some discussion. Conclusions on U(1) are drawn from the Z_6 model at low and intermediate β.

II. THE MODELS AND THE METHOD

We work on a four-dimensional hypercubical lattice. On each site i we have a spin variable S_i taken from the group Z_M,

$$S_i \in Z_M = \{e^{2\pi i m/M} \,|\, m = 1, \ldots, M\}. \tag{2.1}$$

For each pair of nearest-neighbor sites i and j we have a gauge or link variable U_{ij} in the group Z_N,

$$U_{ij} \in \{e^{2\pi i n/N} \,|\, n = 1, \ldots, N\}. \tag{2.2}$$

We require that the quotient

$$l = N/M \tag{2.3}$$

be an integer so that Z_M is a subgroup of Z_N. The link variables are oriented in the sense that

$$U_{ij} = U_{ji}^{*}. \tag{2.4}$$

The dynamics of this system of spin and gauge degrees of freedom follows from the action

$$\mathcal{S} = \beta_H \sum_{(i,j)} \mathcal{S}_L(i,j) + \beta \sum_{\square} \mathcal{S}_{\square}. \tag{2.5}$$

The first sum is over all nearest-neighbor pairs of sites (i,j) where each such pair contributes

$$\mathcal{S}_L(i,j) = 1 - \mathrm{Re}(S_i U_{ij}^{l} S^{-1}{}_j), \tag{2.6}$$

where the power l is defined in Eq. (2.3). The second sum in Eq. (2.5) is over all elementary squares or plaquettes, each such square contributing

$$1 - \mathrm{Re}(U_{ij} U_{jk} U_{kl} U_{li}), \tag{2.7}$$

where the sites i, j, k, and l circulate around the square $\square$. A nearest-neighbor pair contributes to the action a number from the interval $[0, 2\beta_H]$ and a plaquette contributes from $[0, 2\beta]$.

We insert this action into a path integral or partition function

$$Z = \sum_{S_i, U_{ij}} e^{-\mathcal{S}}, \tag{2.8}$$

where the sum is over all allowed configurations of the link and site variables. The free energy of the system is defined as

$$F=\frac{1}{N_S}\ln Z, \tag{2.9}$$

where N_S is the number of sites in the lattice. The correlation functions we study are the average link and average plaquette defined by

$$L=\langle \mathcal{S}_L(i,j)\rangle=-\frac{1}{4}\frac{\partial}{\partial\beta_H}F(\beta,\beta_H), \tag{2.10}$$

$$P=\langle \mathcal{S}_\square\rangle=-\frac{1}{6}\frac{\partial}{\partial\beta}F(\beta,\beta_H). \tag{2.11}$$

The factors $\frac{1}{4}$ and $\frac{1}{6}$ are the ratios of the number of sites to the number of links and plaquettes, respectively, in a four-dimensional lattice.

This system possesses a local gauge symmetry. Given an element g_i of Z_N associated with each site of the lattice, the action is unchanged by the replacement

$$\begin{aligned} &U_{ij}\to g_i U_{ij} g^{-1}{}_j,\\ &S_i\to S_i g^{-1}{}_i. \end{aligned} \tag{2.12}$$

Note that by selecting $g^1{}_i=S_i$ the spin variables all become unity. For gauge-invariant correlation functions the theory is thus equivalent to the pure gauge theory coupled to a non-gauge-invariant applied field of strength β_H. We call this choice the unitary gauge. It will be useful in the discussion of the small-β and the large-β_H limits of the theory.

Even for extremely modest lattice sizes, it is impractical to evaluate the sum in Eq. (2.8) directly. For Z_2 gauge and Higgs fields on a mere 2^4-site lattice this sum has already

$$2^{5\times 2^4}=1.2\times 10^{24} \tag{2.13}$$

terms. Indeed, this immoderate sum suggests a statistical treatment. The Monte Carlo method generates a sequence of states which simulates an ensemble of configurations in thermal equilibrium. In this ensemble the probability of finding a given configuration is proportional to the Boltzmann factor $e^{-\mathcal{S}}$. Expectation values in the states of this sequence should then fluctuate about the true correlation function of the full path integral.

We use a Monte Carlo algorithm which is equivalent to successively placing a heat bath in contact with the individual spins and links of the lattice. After touching any particular spin variable S_i, we replace it with a new value S_i' in a random manner weighted by the Boltzmann factor

$$B=\exp[-\mathcal{S}(S_i')], \tag{2.14}$$

where $\mathcal{S}(S_i')$ is the action evaluated with site i having spin S_i' and all other dynamical variables fixed at their previous values. We similarly treat the link variables. In the remainder of this paper, one Monte Carlo iteration refers to one application of this algorithm to every link and spin variable in the lattice.

For initial configurations we set all $S_i=1$ and set the links either randomly or to unity. (A situation where both site and link variables are random is gauge equivalent to random links and ordered spins.) These two initial states represent infinite and zero temperature. A measure of equilibrium is the agreement of correlation functions obtained with Monte Carlo iterations from these two initial conditions.

The phase diagrams of Sec. IV follow from simulations on a $5\times5\times5\times5$ lattice. We then check a few points in crucial regions on an 8^4 lattice. To minimize surface effects we always impose periodic boundary conditions. Although gauge invariance theoretically permits us to fix spins and only vary links, we have found that convergence of the Monte Carlo procedure is enhanced when the gauge is allowed to fluctuate. In addition to running at fixed β and β_H we have found it useful to adjust β and/or β_H after each iteration to search for values giving a desired average plaquette and/or average link. This allows a rapid determination of contours of constant correlation.

III. LIMITING REGIONS

We now discuss the four limits $\beta_H\to 0,\ \infty$ and $\beta\to 0,\ \infty$. For vanishing β_H the site spins randomize and the model reduces to pure Z_N gauge theory. For $N=2$ this model has a first-order phase transition at the self-dual[1] point $\beta=\frac{1}{2}\ln(1+\sqrt{2})=0.44\ldots$. For Z_6 we have two higher-order transitions occurring at[2]

$$\begin{aligned} &\beta_1=1.00\pm0.01,\\ &\beta_2=1.61\pm0.04. \end{aligned} \tag{3.1}$$

In Figs. 1 and 2 we show the average plaquette

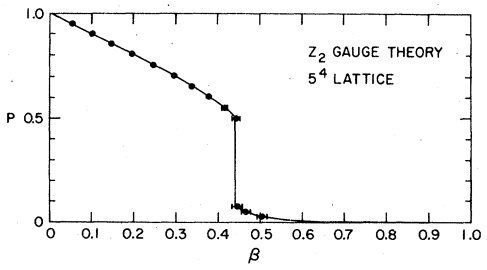

FIG. 1. The average plaquette as a function of β for pure Z_2 gauge theory. The solid line represents the series results in Ref. 1.

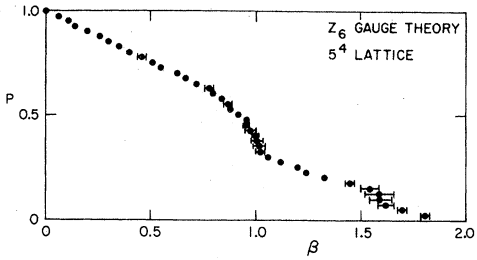

FIG. 2. The average plaquette as a function of β for pure Z_6 gauge theory.

as a function of β for the groups Z_2 and Z_6. Although in Refs. 1 and 2 we used larger lattices, this simulation shows the typical fluctuations expected on a 5^4 lattice. In Ref. 2 a study of lattice size showed no qualitative changes down to a 3^4 lattice; only the fluctuations grew as the size was reduced. In Fig. 1 we also show the series results for Z_2 quoted in Ref. 1.

When $\beta_H \to \infty$ the system must have vanishing average link L. In the unitary gauge this is equivalent to

$$U_{ij}^{l} = 1. \tag{3.2}$$

If the Higgs field is in the fundamental representation, i.e., if $l=1$, the gauge fields must order and both P and L will vanish. However, if $l \neq 1$ then Eq. (3.2) only implies that all gauge variables lie in the quotient group $Z_N/Z_M = Z_l$. Thus as $\beta_H \to \infty$ the theory goes over to a pure Z_l gauge theory. Our treatment of Z_6 gauge fields coupled to Z_3 spins will reduce to Z_2 gauge theory in this limit.

The limit $\beta \to 0$ is trivial in the unitary gauge. Without the gauge interaction the link variables decouple and the average link is

$$L = -\frac{\partial}{\partial \beta_H} \ln\left(\sum_{U \in Z_N} \exp\{-\beta_H [1 - \mathrm{Re}(U^l)]\} \right). \tag{3.3}$$

As each link is decoupled from the others, the average plaquette is

$$P = 1 - (1-L)^4 \, \delta_{l,1}. \tag{3.4}$$

In Fig. 3 we plot the functions in Eqs. (3.3) and (3.4) as a function of β_H for the group Z_2. For comparison, we superpose Monte Carlo results obtained without gauge fixing on a 5^4 lattice.

Finally we come to the limit $\beta \to \infty$. Here all plaquettes must go to the identity. The gauge fields are then gauge equivalent to total ordering and the model reduces to a pure Z_M spin system with nearest-neighbor couplings. In Fig. 4 we show the results of simulations of this system with Z_2 Higgs fields. The Z_2 model is the Ising[7] model and the Z_3 model is equivalent to the three-state Potts[8] model, both in four dimensions. These

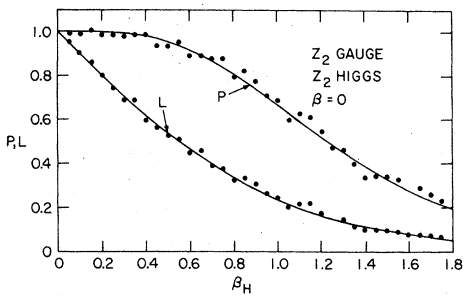

FIG. 3. The average plaquette and link as a function of β_H for the Z_2 system at $\beta = 0$. The solid lines are the exact result and the points are from Monte Carlo simulation.

systems all exhibit ferromagnetic phase transitions. Based on mean-field theory, conventional lore is that for Z_2 and Z_6 these transitions are second order. For Z_3, however, there is appreciable evidence that this is a first-order phase transition.[9] The inverse temperatures of these transitions are

$$\beta_H = \begin{cases} 0.150 \text{ for } Z_2 \\ 0.258 \text{ for } Z_3 \\ 0.34 \pm 0.01 \text{ for } Z_6. \end{cases} \tag{3.5}$$

The values for Z_2 and Z_3 are from Refs. 9 and 10, while for Z_6 we used our own analysis on an 8^4 lattice.

To summarize this section, the models under study have one or two transition lines entering the phase diagram from the axis $\beta_H = 0$, one transition at $\beta = \infty$ and zero or one transition at $\beta_H = \infty$. In the next section we will see how these lines connect in the interior of the diagram. The figures in the present section serve to indicate the typical fluctuations occurring in Monte Carlo simulations on a 5^4 lattice.

IV. THE DIAGRAMS

In Fig. 5 we show contours of constant L and P in the (β, β_H) plane for the gauge group Z_2 and

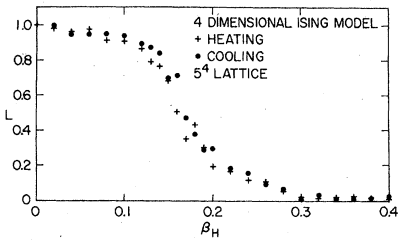

FIG. 4. A thermal cycle on the four-dimensional Ising model. Each point is the average link after 10 iterations at fixed β_H. At each β_H the lattice was started in the configuration obtained from an adjacent point, either hotter or cooler.

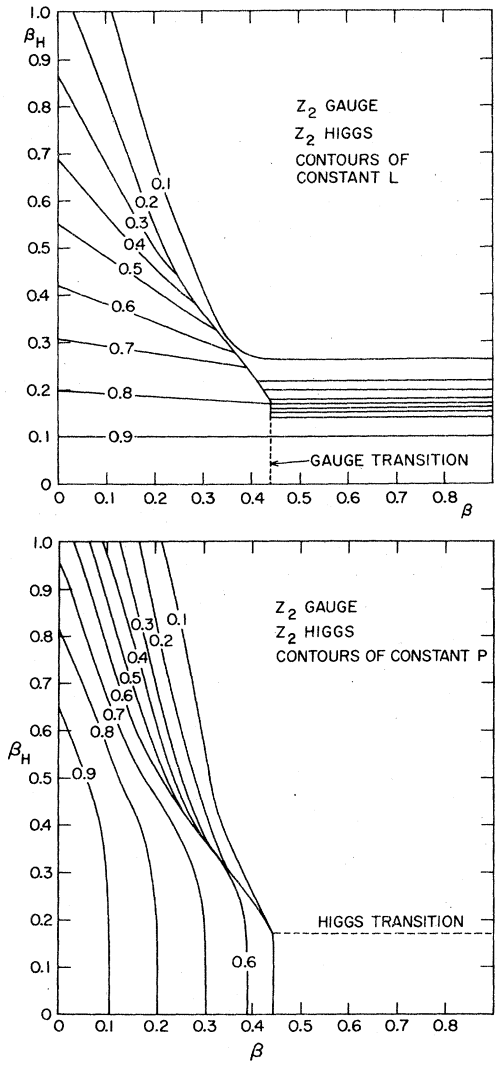

FIG. 5. Contours of constant L and P for Z_2 gauge theory coupled to Z_2 Higgs fields.

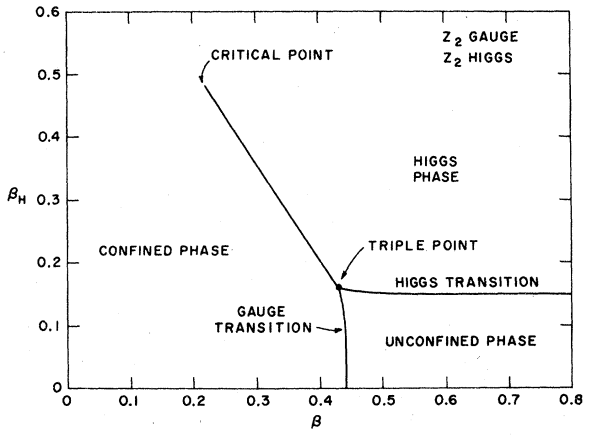

FIG. 6. Summary of the Z_2 phase diagram.

Higgs field also in Z_2. The trajectory of the gauge transition through the diagram is apparent as a "cliff" in the values of P and L. The Higgs transition appears as a steep "hill" in the value of L. This hill disappears beneath the cliff at a triple point. The first-order line continues into the diagram until it unfolds at a critical point. Beyond that critical point the system appears smooth as predicted in Ref. 6. Figure 6 summarizes the general features of the phase diagram.

As gauge fluctuations induce disorder, the Higgs transition should move to larger β_H as β is reduced.[6] However, the gauge field is so thoroughly

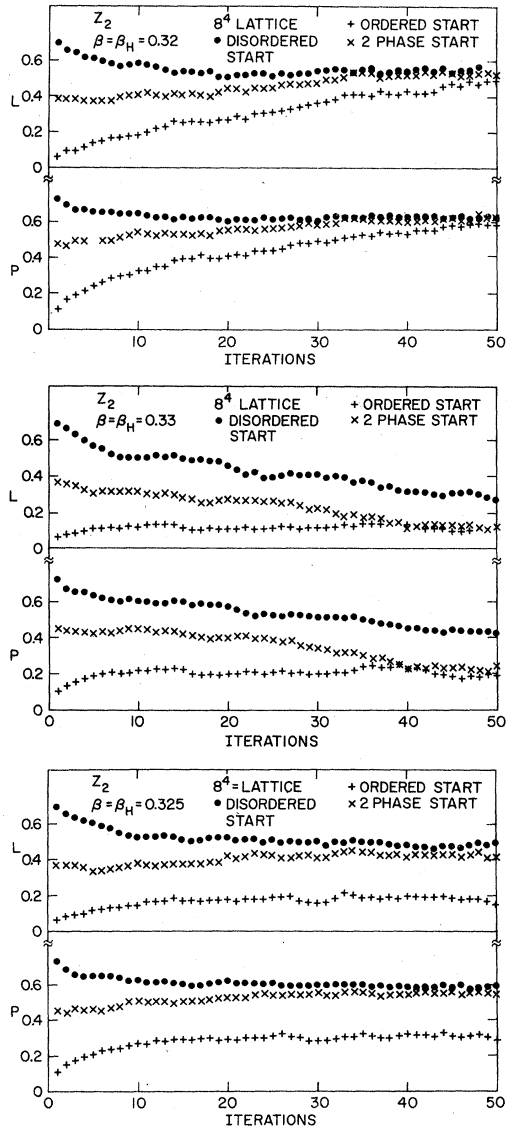

FIG. 7. Fifty iterations on an 8^4 lattice for the Z_2 system at (a) $\beta=\beta_H=0.32$, (b) $\beta=\beta_H=0.33$, and (c) $\beta=\beta_H=0.325$.

ordered for $\beta > 0.44$ that we cannot see this shift. Similarly the gauge transition should move to lower β as β_H is increased, but below the triple point this shift is also too small to appear in our analysis. Thus we place the triple point at $\beta = 0.43 \pm 0.02$, $\beta_H = 0.16 \pm 0.02$.

In Fig. 7 we show the average plaquette and link as a function of number of Monte Carlo iterations on an 8^4 lattice with β and β_H chosen near the transition line above the triple point. These runs were initiated with three distinct starting conditions, ordered, disordered, and a mixed phase. In the latter, half the lattice was ordered and half random. Such a state should evolve without being caught in a metastable phase associated with a first-order phase transition. Figure 7(a) shows that the point $\beta = \beta_H = 0.32$ lies on the disordered side of the transition line while Fig. 7(b) shows $\beta = \beta_H = 0.33$ is ordered. The first-order nature of the line is manifest in Fig. 7(c), where at $\beta = \beta_H = 0.325$ two stable phases appear and the mixed phase drifts rather slowly. The critical point where this first-order line terminates is difficult to locate precisely because of the steep behavior beyond it. We estimate $\beta = 0.22 \pm 0.03$ and $\beta_H = 0.48 \pm 0.03$ as its coordinates.

In Fig. 8 we show contours of P and L for the gauge group Z_6 with the Higgs field in the fundamental representation. The Higgs transition again appears as a steep slope in L. For β_H below this transition P is essentially independent of β_H.

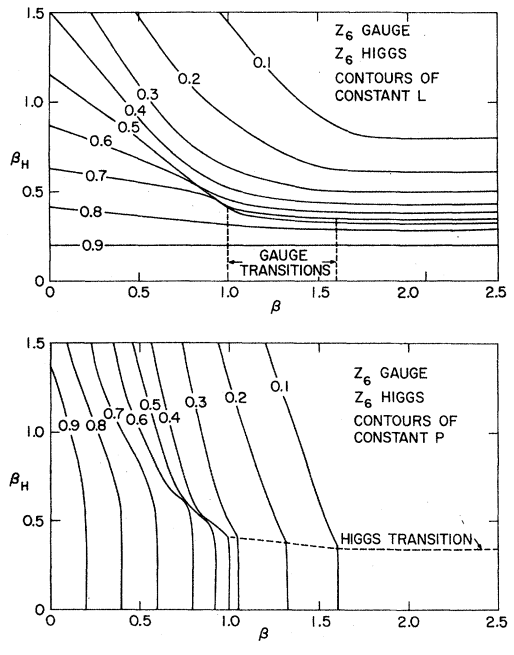

FIG. 8. Contours of constant L and P for the coupled Z_6 spin-gauge system.

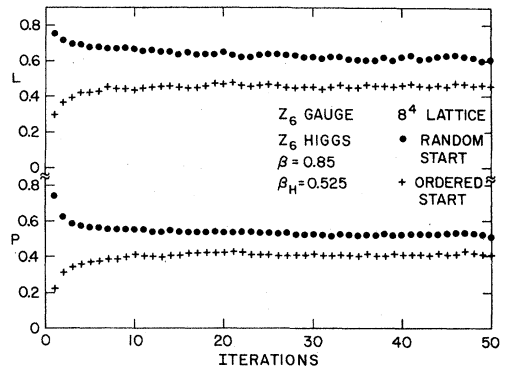

FIG. 9. Fifty iterations on an 8^4 lattice for the coupled Z_6 system at $\beta = 0.85$, $\beta_H = 0.525$.

The two gauge transitions thus proceed essentially at constant β until they join the Higgs transition at two separate triple points. For β below the junction of the Higgs and high-temperature gauge transitions, we have a single transition line terminating at a critical point similar to that seen with Z_2. This line appears to be first order, but this is not certain because the discontinuity across it is less substantial than in the Z_2 case. For the large-β triple point we quote

$$\beta = 1.60 \pm 0.05, \quad \beta_H = 0.35 \pm 0.02, \tag{4.1}$$

and for the low-β triple point

$$\beta = 0.98 \pm 0.03, \quad \beta_H = 0.42 \pm 0.03. \tag{4.2}$$

The location of the critical point is

$$\beta = 0.67 \pm 0.05, \quad \beta_H = 0.67 \pm 0.05. \tag{4.3}$$

The errors in the above numbers are subjective estimates. To argue that the line connecting the critical point with the low-β triple point is first order, we show in Fig. 9 runs on an 8^4 lattice at $\beta = 0.85$, $\beta_H = 0.525$ with both random and ordered

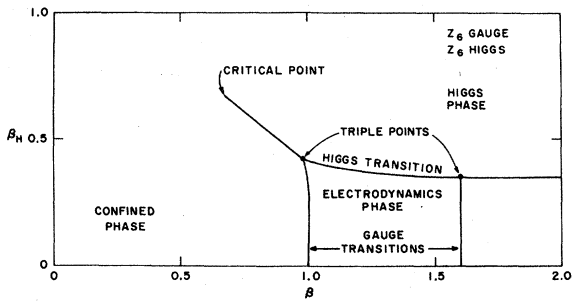

FIG. 10. Phase diagram for the Z_6 system.

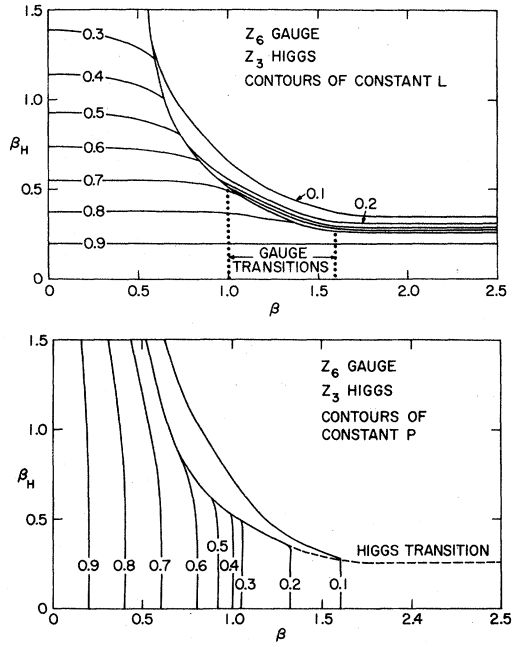

FIG. 11. Contours of constant L and P for Z_6 gauge fields coupled to Z_3 Higgs fields.

initial states. These runs appear to yield distinct phases, but the separation is small. The general features of the phase diagram for this system are summarized in Fig. 10.

Finally, in Fig. 11 we plot the P and L contours for Z_6 gauge fields with the Higgs field in the Z_3 representation. Qualitatively the diagram is similar to that seen in Fig. 8 except that the first-order line with β_H above the low-β triple point no longer unfolds. Rather it continues to large-β_H and becomes the first-order transition of the residual Z_2 theory. Both triple points are shifted to lower β_H because the Z_3 spin system is naturally more ordered than Z_6. The large-β triple point occurs at

$$\beta_H = 1.58 \pm 0.05\,, \qquad \beta_H = 0.28 \pm 0.02\,, \tag{4.4}$$

while the other occurs at

$$\beta = 0.98 \pm 0.03\,, \qquad \beta_H = 0.51 \pm 0.03\,. \tag{4.5}$$

This phase diagram is summarized in Fig. 12.

V. DISCUSSION

We have experimentally studied the phase diagrams for Z_2 and Z_6 gauge theories coupled to Higgs fields. Since Z_6 pure gauge theory behaves

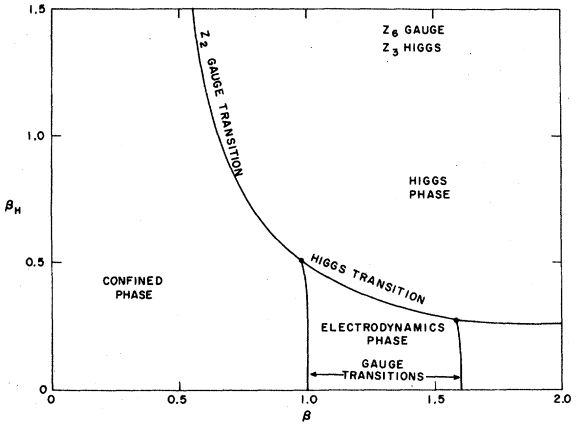

FIG. 12. Phase diagram for the Z_6 gauge, Z_3 spin system.

essentially as the U(1) model for β below the second transition,[2] the first triple point and the unfolding of a first-order line are likely properties of a similar phase diagram for the U(1) coupled Higgs-gauge system. The lack of unfolding for Z_3 site spins coupled to Z_6 gauge fields corresponds to the case of a doubly charged Higgs field in the U(1) system. This work confirms the basic structure of these phase diagrams as predicted in Ref. 6.

Except for the Z_3 case, when β is infinite the Higgs transition is second order. An interesting question is whether this critical point is part of a line of second-order transitions or if the Higgs transition becomes first order in the interior of the diagram. We cannot answer this with our crude Monte Carlo results because when the gauge fields are ordered the effect of β on the Higgs transition is slight.

It might seem remarkable that we can obtain information from a lattice as small as five sites on a side. Note, however, that the number of states for such a system is extremely large; for the Z_2 case there are

$$2^{5^4 \times 5} = 5.23 \times 10^{940}$$

distinct configurations. This large number supports a statistical treatment. Also note that we have only asked rather crude questions about the location of transitions; more subtle points such as critical exponents presumably require considerably more detailed analysis on larger lattices.

ACKNOWLEDGMENT

This work was supported by the U. S. Department of Energy under Contract No. EY-76-C-02-0016.

[1]M. Creutz, L. Jacobs, and C. Rebbi, Phys. Rev. Lett. 42, 1390 (1979).
[2]M. Creutz, L. Jacobs, and C. Rebbi, Phys. Rev. D 20, 1915 (1979).
[3]M. Creutz, Phys. Rev. Lett. 43, 553 (1979).
[4]P. Higgs, Phys. Rev. Lett. 13, 508 (1964).
[5]S. Elitzur, R. B. Pearson, and J. Shigemitsu, Phys. Rev. D 19, 3698 (1979); A. Ukawa, P. Windey, and A. H. Guth, Phys. Rev. D (to be published).
[6]R. Balian, J. Drouffe, and C. Itzykson, Phys. Rev. D 10, 3376 (1974); E. Fradkin and S. Shenker, *ibid.* 19, 3682 (1979); T. Banks and E. Rabinovici, Institute for Advanced Study report, 1979 (unpublished).
[7]E. Ising, Z. Phys. 31, 253 (1925).
[8]R. B. Potts, Proc. Cambridge Philos. Soc. 48, 106 (1952).
[9]H. Blöte and R. Swendsen, Phys. Rev. Lett. 43, 799 (1979).
[10]M. E. Fisher and D. S. Gaunt, Phys. Rev. 133, A224 (1964).